Disintegration of Hyperfragments. III*

J. SCHNEPS, *Department of Physics, Tufts University, Medford, Massachusetts*

AND

W. F. FRY AND M. S. SWAMI, *Department of Physics, University of Wisconsin, Madison, Wisconsin*

(Received February 20, 1957)

The systematic study of hyperfragments using nuclear emulsion, which has been reported on in two previous papers, has been continued. Examples of ${}_\Lambda H^4$, ${}_\Lambda He$, and ${}_\Lambda Li$ hyperfragments are reported here. Λ^0 particle binding energies previously reported have been corrected according to the latest range-energy data of Barkas *et al.* Average values found for the binding energy B_Λ are:

${}_\Lambda H^3(B_\Lambda=-0.3\pm0.4$ Mev); ${}_\Lambda H^4(B_\Lambda=1.8\pm0.4$ Mev); ${}_\Lambda He^4(B_\Lambda=1.9\pm0.4$ Mev); ${}_\Lambda He^5(B_\Lambda=1.6\pm0.6$ Mev); ${}_\Lambda Li^6(B_\Lambda=6.8\pm3.0$ Mev); ${}_\Lambda Li^6$ or ${}_\Lambda Li^7(B_\Lambda=5.2$ or 5.0 ± 2.5 Mev); ${}_\Lambda Li^7$ or ${}_\Lambda Li^8(B_\Lambda=5.1\pm0.6$ Mev); ${}_\Lambda Be^8(B_\Lambda=5.1\pm4.0$ Mev); ${}_\Lambda Be^9(B_\Lambda=6.2\pm0.6$ Mev); ${}_\Lambda C^{11}(B_\Lambda=13\pm6$ Mev).

The absence of ${}_\Lambda H^2$ indicates the Λ^0-nucleon system does not have a bound state. The absence of ${}_\Lambda He^3$ implies that ${}_\Lambda H^3$ is an isotopic spin singlet. The agreement in the binding energies of ${}_\Lambda H^4$ and ${}_\Lambda He^4$ supports the hypothesis of charge independence for Λ^0-nucleon forces. The ratios of nonmesonic to mesonic decays of hyperfragments $Q^{(-)}$, as defined by Ruderman and Karplus, are found to be: for hydrogen hyperfragments $Q^{(-)}=0$; for helium $Q^{(-)}=1.5$; for hyperfragments of $Z\geqslant3$, $Q^{(-)}=43$. According to the analysis of Ruderman and Karplus these values suggest that the Λ^0 particle decays into an angular momentum state of $l=0$ or $l=1$, and hence that the spin of the Λ^0 is either $\frac{1}{2}$ or $\frac{3}{2}$. In the case of hyperfragments which decay into a proton, π^- meson, and a recoil, the angle $\theta_{\Lambda\pi}$ between the π^--meson direction in the Λ^0 rest frame and the direction of motion of the Λ^0 within the hyperfragment can be measured, if it is assumed that the interaction of the decay particles is negligible. The distribution of these angles shows a peaking in the forward and backward directions. This is suggestive of a spin greater than $\frac{1}{2}$ for the Λ^0.

INTRODUCTION

THE data on hyperfragment decays yield information on the interaction between the Λ^0 particle and nucleons,[1–3] and also, with the aid of certain theoretical considerations, on the intrinsic properties of the Λ^0 particle, i.e., spin, parity, and isotopic spin. For example, Ruderman and Karplus[4] and Primakoff[5] have shown how the data on nonmesonic to mesonic decay ratios for hyperfragments may be applied to obtain information on the spin of the Λ^0. If the Λ^0 particle is, as has been suggested,[6] a parity doublet, this too should be reflected in the values of these ratios.[7] Angular correlations in the mesonic decays of hyperfragments may also yield information on the spin.[8] Dalitz[9] and Jones and Knipp[10] have pointed out that if charge independence holds for hyperfragments, then the observation of charge multiplets whose members have equal binding energies for the Λ^0 would verify the assignment of $T=0$ for the isotopic spin of the Λ^0.

The data on hyperfragments which were previously reported on in two papers, henceforth to be referred to as I[11] and II,[12] have been expanded and the further results are reported here.

PROCEDURE

Pellicle stacks were exposed to cosmic rays and to 3-Bev π^- mesons, and K^- mesons[13] from the Berkeley bevatron. The methods for finding and identifying hyperfragments were the same as reported in I and II.

OBSERVATIONS

A. Production of Hyperfragments

Since I and II, 42 hyperfragments were found from 48000 3-Bev π^- stars, 33 from 78000 cosmic-ray stars, and 35 from 795 K^- stars. The data on hyperfragment production frequencies from I, II, and III are combined in Table I. As previously pointed out, some of the events may be the result of the capture of slow π^- mesons. However, if the range of the connecting track is greater than 15 microns, a fragment generally can be distinguished from a π^- meson. Such events are also included in Table I. The results of Fry and Wold,[14] who studied the range distribution of π^- mesons from interactions where the incident energy was below the threshold for Λ^0 production, suggests that few of the short-range events listed as hyperfragments here, could have been due to slow π^- mesons. It is not surprising that many hyperfragments have a very short range since most of them have a charge greater than 3 and thus a high rate of energy loss.

The charge distribution of all the hyperfragments listed in Table I is given in Fig. 1 and the charge dis-

* Supported in part by the U. S. Atomic Energy Commission and by the Graduate School from funds supplied by the Wisconsin Alumni Research Foundation.

[1] R. H. Dalitz, *Proceedings of the Sixth Annual Rochester Conference* (Interscience Publishers, Inc., New York, 1956).
[2] J. T. Jones, Jr., and J. M. Keller, Nuovo cimento **4**, 1329 (1956).
[3] D. B. Lichtenberg and M. Ross, Phys. Rev. **103**, 1131 (1956).
[4] M. Ruderman and R. Karplus, Phys. Rev. **102**, 247 (1956).
[5] H. Primakoff, Nuovo cimento **3**, 1394 (1956).
[6] T. D. Lee and C. N. Yang, Phys. Rev. **102**, 290 (1956), and **104**, 822 (1956).
[7] S. B. Treiman, Phys. Rev. **104**, 1475 (1956).
[8] P. Zielinski, Nuovo cimento **3**, 1479 (1956).
[9] R. H. Dalitz, Phys. Rev. **99**, 1475 (1955).
[10] J. T. Jones, Jr., and J. K. Knipp, Nuovo cimento **2**, 857 (1955).
[11] Fry, Schneps, and Swami, Phys. Rev. **99**, 1561 (1955).
[12] Fry, Schneps, and Swami, Phys. Rev. **101**, 1526 (1956).
[13] Fry, Schneps, Snow, Swami, and Wold (to be published).
[14] W. F. Fry and D. C. Wold, Phys. Rev. **104**, 1478 (1956).

TABLE I. Frequencies of hyperfragments.

Nature of exposure	1.5-Bev π^--mesons	3-Bev π^--mesons	3-Bev protons	6-Bev protons	Cosmic rays	K^--meson stars
Number of stars observed	500	80000	20000	10000	119000	1001
Total number of hyperfragments	1	72	19	7	61	46
Number of hyperfragments with $R \geq 15\,\mu$	0	19	3	3	19	9
Ratio of all hyperfragments to total stars	2×10^{-3}	9×10^{-4}	9.5×10^{-4}	7×10^{-4}	5.1×10^{-4}	4.6×10^{-2}
Ratio of hyperfragments with $R \geq 15\,\mu$ to total stars	0	2.4×10^{-4}	1.5×10^{-4}	3×10^{-4}	1.6×10^{-4}	9×10^{-3}

tribution of those with range greater than 15 microns is given in Fig. 2. The range distribution of all hyperfragments is given in Fig. 3.

B. Measurable Events

In this section are described π^--mesonic decays, events in which the binding energy of the Λ^0 could be measured, and events which could be interpreted as π^0-mesonic decays. The range-energy relations of Barkas and co-workers[15] was used for singly charged particles in all cases, and that of Wilkins[16] for multiply charged particles.

Event 133

This hyperfragment emerged from a cosmic-ray star. Its range was 1410 microns and the characteristics of its track showed its charge was one. A multiple scattering measurement along the track gives a mass of $(6300_{-1600}{}^{+5200})m_e$ for the hyperfragment. The hyperfragment decayed into three charged particles whose tracks are coplanar. A summary of the measurements is given in Table II and a drawing of the event is shown in Fig. 4. The requirement of momentum balance identifies tracks 1 and 2 as due to a proton and triton, respectively. Any other assumptions lead to a large momentum unbalance. The disintegration scheme can be written

$$_{\Lambda}H^4 \rightarrow p + t + \pi^- + Q,$$

where $Q = 35.1 \pm 0.3$ Mev. The binding energy of the Λ^0 particle in $_{\Lambda}H^4$ is then 1.8 ± 0.4 Mev. It is to be noted that the identification of this fragment from its decay is consistent with the scattering measurement on its track.

Event 143

This hyperfragment was produced by a 3-Bev π^- meson. Its range was 138 microns and it decayed into three particles, a π^- meson and a proton whose tracks make an angle of 171°, and a short recoil of range about 1.3 microns. Unfortunately the π-meson track could not be followed to its end, but its energy was found from grain density to be about 30 Mev. The residual momentum of the proton and π meson is 16 Mev/c. Only a hydrogen recoil of this momentum would have a range as large as 1.3 microns. Therefore this event is interpreted as the mesonic decay of $_{\Lambda}H^3$ or $_{\Lambda}H^4$.

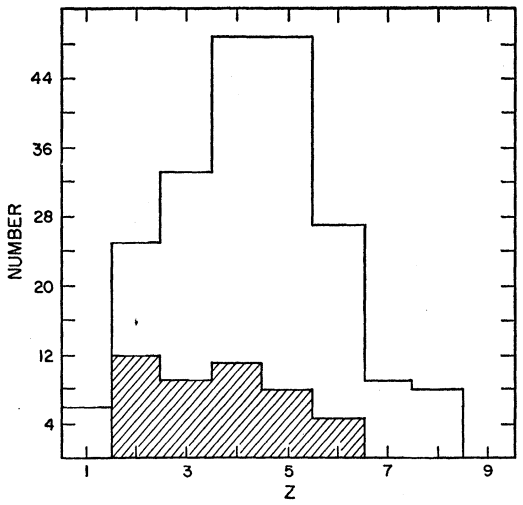

FIG. 1. The charge distribution of hyperfragments. The shaded area represents hyperfragments from K^- stars.

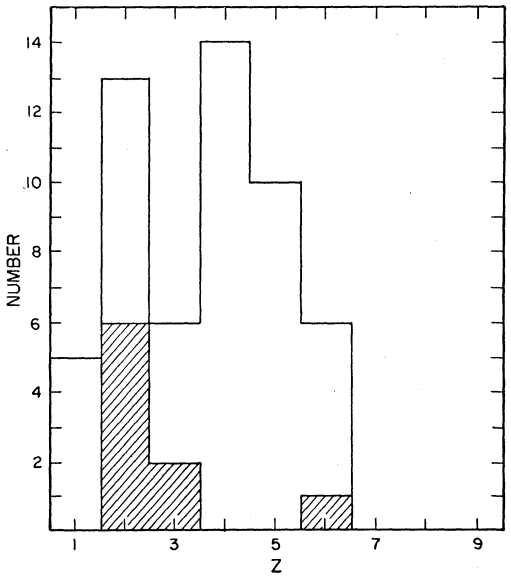

FIG. 2. The charge distribution of hyperfragments whose range is greater than 15 microns. The shaded area represents hyperfragments from K^- stars.

[15] Barkas, Barrett, Cuer, Heckman, Smith, and Ticho, University of California Radiation Laboratory Report UCRL-3254 (unpublished). W. H. Barkas, University of California Radiation Laboratory Report UCRL-3384 (unpublished).

[16] J. J. Wilkins, Atomic Energy Research Establishment, Harwell Report G/R664 (unpublished).

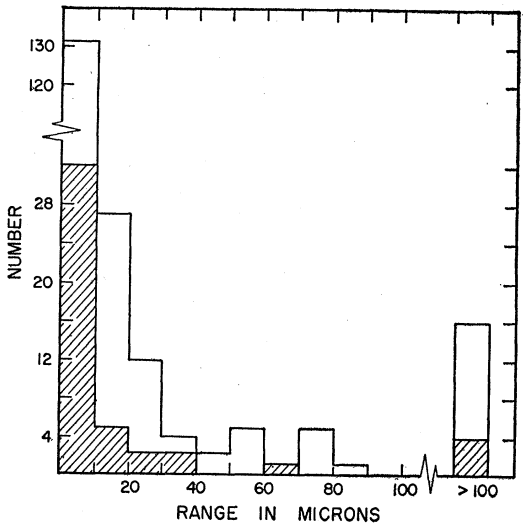

FIG. 3. The range distribution of hyperfragments. The shaded area represents hyperfragments from K^- stars.

Event 190

This hyperfragment came from a star produced by a stopped K^- meson. The measurements are summarized in Table III.

The three tracks from the decay are coplanar within the error in measurement. However track 2 is steep and its projected length is only 2.2 microns. Therefore it is difficult to measure its dip angle accurately. An accurate value for the dip angle can be obtained by assuming track 2 is in the direction of the residual momentum of tracks 1 and 3, assuming track 1 to be due to a proton. Then track 2 is found to have a dip angle of 71° and a range of 7.1 microns.[17] When this value for the range is used, momentum is balanced by assuming track 2 to be due to He^3. It should be pointed out that if the range were 5 microns then He^4 would balance momentum. Any other assumption for track 1 other than a proton is inconsistent with the data. The most likely interpretation is then

$$_{\Lambda}He^4 \rightarrow He^3 + p + \pi^- + Q,$$

where $Q = 34.6 \pm 0.5$ Mev. The binding of the Λ^0 then is 2.3 ± 0.6 Mev.

TABLE II. Measurements on event 133.

Track	Range in microns	Identity	Energy in Mev	Angles in decay plane
Hyper-fragment	1410	$_{\Lambda}H^4$	33.0	
1	1120	p	14.9	160°
2	82	t	4.7	
3	4921	π^-	15.5±0.3	96°

[17] This result only holds if the normal shrinkage factor of an emulsion can be applied to tracks which are both very short and very steep. It is possible that this may not be the case.

Event 213

This hyperfragment also came from a K^- star. Its range was only about one micron. It decayed into two particles, one a proton (track 1) of range 2.79 cm and the other a singly charged particle (track 2) of range 790 microns. The measurements on this event are given in Table IV.

If track 2 is assumed to have been made by a deuteron and it is assumed that only one neutron was emitted from the decay, the energy of the neutron is 57.3 ± 2.4 Mev. The decay scheme is

$$_{\Lambda}He^4 \rightarrow p + d + n + Q,$$

where $Q = 167.5 \pm 2.6$ Mev and the binding of the Λ^0 is 2.1 ± 2.6 Mev.

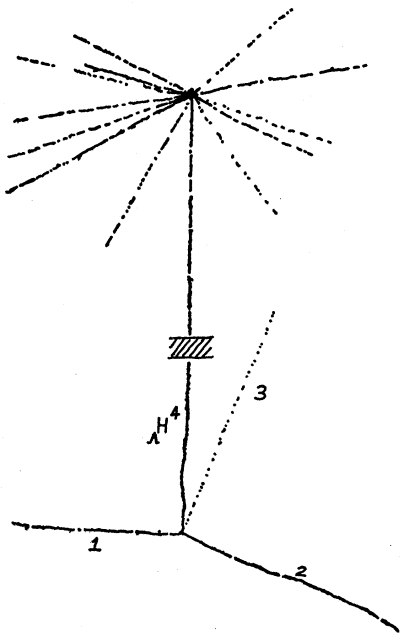

FIG. 4. A $_{\Lambda}H^4$ hyperfragment (event 133) from a large cosmic-ray star decayed after coming to rest into a proton (1), a triton (2), and a π^- meson (3).

If one assumes that only one neutron was emitted, no other decay scheme is consistent with known data on binding energies.

Event 186

The range of this hyperfragment, which originated from a K^- star, was 102 microns. The measurements on this event are summarized in Table V.

The three tracks from the decay are coplanar within the error of measurement. The best value for the range of track 2 is 2.0 ± 0.5 microns. If the residual momentum of the proton and π^- meson is given to a He^3 or a He^4 nucleus, their expected ranges would be 2.9 microns and 2.7 microns, respectively. Thus one cannot distinguish between these two. The disintegration could

have been either

$$_{\Lambda}He^{4}\rightarrow He^{3}+p+\pi^{-},$$

or

$$_{\Lambda}He^{5}\rightarrow He^{4}+p+\pi^{-}.$$

The binding energies for these two possibilities are 3.3±0.6 Mev and 3.2±0.6 Mev.

Event 188

A stopped K^{-} meson produced this hyperfragment. The data are summarized in Table VI.

The only visible tracks from the decay are 1 and 2. However, the emission of one or more neutrons is not consistent with a hyperfragment decay, since it leads to negative binding energies for the Λ^{0} particle. It turns out, that if track 2 is due to a proton, the residual momentum vector of the proton and π^{-} meson lies directly underneath the hyperfragment track, and its magnitude is 39 Mev/c. A recoil of length less than 2 microns would be masked by the hyperfragment track. A triton recoil would have a range of 3 microns, whereas He^{3} and He^{4} would both have a range of about 1.5 microns. It seems likely then that the decay scheme was either

$$_{\Lambda}He^{4}\rightarrow He^{3}+p+\pi^{-},$$

or

$$_{\Lambda}He^{5}\rightarrow He^{4}+p+\pi^{-},$$

with binding energies for the Λ^{0} of 2.0±0.6 Mev and 2.1±0.6 Mev, respectively. If the recoil were heavier than He^{4}, then the binding energy, as will be seen later, would not be consistent with values found for heavier hyperfragments.

TABLE III. Measurements on event 190.

Track	Range in microns	Identity	Energy Mev	Angles in decay plane
Hyper fragment	200	$_{\Lambda}He^{4}$	20.5	
1	15.1	p	1.1	113°
2	7.1	He^{3}	2.0	154°
3	16825	π^{-}	31.5±0.5	

TABLE IV. Measurements on event 213.

Track	Range in microns	Identity	Energy in Mev	Angle in degrees
Hyper-fragment	1	$_{\Lambda}He^{4}$		
1	27900	p	94.2±0.8	129.7±1.8
2	790	d	16.0±0.3	
E_n=57.3±2.4 Mev				

Event 211

A negative K star was the source of this hyperfragment whose range was 111 microns. From the appearance of its track the charge of the hyperfragment is estimated to have been 1 or 2. It decayed into a proton, π meson, and a recoil, but unfortunately the π meson left the emulsion stack so that its energy had to be determined from its grain density. The measurements on this event are given in Table VII.

TABLE V. Measurements on event 186.

Track	Range in microns	Identity	Energy in Mev	Angles in decay plane
Hyper-fragment	102	$_{\Lambda}He^{4}$ or $_{\Lambda}He^{5}$	13.5 or 17.0	
1	271	p	6.48	128°
2	2.0±0.5	He^{3} or He^{4}	0.49 0.64	85°
3	12570	π^{-}	26.6±0.5	

The residual momentum of the proton and π meson is 120.5±3.5 Mev/c. If the recoil were He^{4}, its momentum would be (from its range) 117±7 Mev/c whereas if it were He^{3}, its momentum would be 103±7 Mev/c. Therefore this event is best interpreted as

$$_{\Lambda}He^{5}\rightarrow He^{4}+p+\pi^{-}+Q,$$

where Q=35.6±1.5 Mev and the binding of the Λ^{0} is 1.3±1.5 Mev.

Event 172

This event occurred in a plate exposed to cosmic rays. The hyperfragment had a range of 5 microns and decayed into three particles which were not coplanar. The data are summarized in Table VIII.

Track 2 could have been due to a particle of charge 1 or 2. Track 3 was produced by a particle of charge 1. A multiple scattering measurement on it gives a mass of $(3150_{-520}^{+850})m_e$, which indicates that it was most likely due to a deuteron. If we assume this and that track 2 was also made by a deuteron, and give the residual momentum to one neutron, the energy of the neutron is 90.5 Mev. The disintegration scheme is

$$_{\Lambda}Li^{6}\rightarrow p+d+d+n+Q,$$

where Q=146.8 Mev and the binding energy of the Λ^{0} particle is 6.8±3.0 Mev.

It should be pointed out that the fit with one neutron may be fortuitous.

Event 123

This hyperfragment was produced by a 3-Bev π^{-} meson. In this case the hyperfragment track was very

TABLE VI. Measurements on event 188.

Track	Range in microns	Identity	Energy in Mev	Angle
Hyper-fragment	36	$_{\Lambda}He^{4}$ or $_{\Lambda}He^{5}$	7.4 or 9.3	
1	17250	π^{-}	32.0	162°
2	59.6	p	2.6	
3	···	He^{3} or He^{4}	0.3 or 0.2	

TABLE VII. Measurements on event 211.

Track	Range in microns	Identity	Energy in Mev	Angles in decay plane
Hyper-fragment	111	${}_\Lambda He^5$	16.3	
1	1495	p	17.7	160°
2	73230	π	16.0±1.5	
3	6.8±1.0	He^4	1.9	31°

long, 985 microns, and the δ rays along it plus the lack of thindown near its end show that the fragment had a charge of three or four. The hyperfragment decay consisted of two tracks. Track 1 was due to a particle of charge one or two and track 2 to a particle of charge one. Since it is known that the fragment charge was three or four, this makes it clear that track 1 was due to either He^3 or He^4. The grain density of track 2 indicates that it was produced by a deuteron. The data on this event are given in Table IX and a drawing is shown in Fig. 5.

If the residual momentum of the two visible decay particles is given to one neutron, then the following two schemes fit a hyperfragment decay:

$$ {}_\Lambda Li^6 \rightarrow He^3 + d + n + Q_1, $$

and

$$ {}_\Lambda Li^7 \rightarrow He^4 + d + n + Q_2, $$

where $Q_1 = 153.9$ Mev and $Q_2 = 168.6$ Mev. If the event was ${}_\Lambda Li^6$, then the binding energy is 5.2±2.5 Mev. If it was ${}_\Lambda Li^7$, the binding energy is 5.0±2.5 Mev.

Again it must be remembered that a fit to one neutron may be fortuitous. For example, the event could have been

$$ {}_\Lambda Li^8 \rightarrow He^4 + d + 2n. $$

Event 164

A cosmic-ray star was the origin of this hyperfragment. The range of the fragment was 27 microns and it decayed into three particles; a π^- meson, a proton, and a recoil of short range whose direction is consistent with coplanarity. The data on this event are summarized in Table X.

The range of the short recoil is difficult to measure. A best estimate is that it lies between 0.5 and 1.3 microns. Since the size of a grain can be as large as 0.5 micron, the exact measurement of the range is not too significant. The residual momentum of the proton and π^- meson is 44 Mev/c. He^3, He^4, Li^6, and Li^7 recoils of this momentum would have ranges of 1.4, 1.3, 0.4, and 0.35 micron, respectively. If the recoil were helium, however, the event would give a binding energy of 4.9±0.6 Mev for ${}_\Lambda He^4$ or ${}_\Lambda He^5$ which is not consistent with the previously determined binding energies for He. Therefore the most likely interpretation is that the disintegration was either

$$ {}_\Lambda Li^7 \rightarrow Li^6 + p + \pi^- + Q_1, $$

or

$$ {}_\Lambda Li^8 \rightarrow Li^7 + p + \pi^- + Q_2, $$

where Q_1 and Q_2 are both 31.8±0.5 Mev and the binding energy of the Λ^0 in either case is 5.1±0.6 Mev.

The only other possibility for this event is that track 1 was due to a deuteron and the decay was

$$ {}_\Lambda Li^9 \rightarrow Li^7 + d + \pi^-. $$

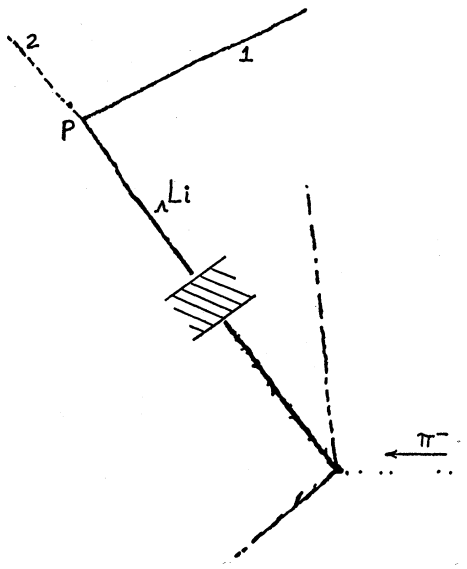

FIG. 5. A ${}_\Lambda Li^6$ or ${}_\Lambda Li^7$ hyperfragment was produced by a 3-Bev π^- meson. After coming to rest it decayed nonmesonically at the point P into a deuteron (2), He^3 or He^4(1), and a neutron (event 123).

TABLE VIII. Data on event 172

Track	Range in microns	Identity	Energy in Mev
Hyperfragment	5	${}_\Lambda Li^6$	2.5
1	4020	p	31.1
2	123	d	5.3
3	1111	d	19.9

However, in this case the binding energy is 3.4 Mev which is considerably less than the 6.2-Mev binding energy which was found for ${}_\Lambda Be^9$. Since the binding energy is probably primarily a function of mass number, this interpretation seems less likely than the other two, although it cannot be ruled out.

Event 167

This event was found in a stack exposed to cosmic rays, but unfortunately it occurred before the pellicle stack was assembled. Hence, those tracks which leave the pellicle cannot be followed. The fragment had a range of 52 microns and decayed into three particles whose trajectories were coplanar. One produced a light track and was presumably a π^- meson. The track of the second particle leaves the stack shortly before stopping

and its total range is estimated to be about 2000 microns. If it was due to a proton, the momentum was about 200 Mev/c. The third track is a recoil of 3 microns. Knowing the angles between the tracks, one can make various assumptions for the decay and test them for consistency with the range of the recoil. The only ones which are consistent are

$$_{\Lambda}\mathrm{Li}^{7}\rightarrow \mathrm{Li}^{6}+p+\pi^{-},$$

and

$$_{\Lambda}\mathrm{Li}^{8}\rightarrow \mathrm{Li}^{7}+p+\pi^{-}.$$

A He recoil should have had a range of about 8 microns and a Be recoil should have had a range of 2 microns. Therefore, this event was most likely the mesonic decay of $_{\Lambda}$Li.

Event 144

This hyperfragment came from a cosmic-ray star. Its track is only 6 microns long but shows a large angle

TABLE IX. Data on event 123.

Track	Range in microns	Identity	Energy in Mev	Angle
Hyper-fragment	985	$_{\Lambda}$Li^{6} or $_{\Lambda}$Li^{7}	104 or 112	
1	233	He^{3} or He^{4}	21.4 or 24.0	120.9°
2	5670[a]	d	51.5	
	E_n=81.0 Mev if $_{\Lambda}$Li^{6} E_n=93.1 Mev if $_{\Lambda}$Li^{7}			

[a] This range should be multiplied by 1.014 to take into account the density of the emulsion, before applying the range-energy relation.

TABLE X. Measurements on event 164.

Track	Range in microns	Identity	Energy in Mev	Angle in decay plane
Hyper-ragment	27	$_{\Lambda}$Li^{7} or $_{\Lambda}$Li^{8}	17.5 or 20.0	
1	136	p	4.28	152°
2	13250	π^{-}	27.4	
3	0.5<R<1.3	Li^{6} or Li^{7}	0.17 or 0.15	140°

scattering just before its end which indicates that the fragment came to rest. There are two decay tracks, both of which are very short. A drawing of this event is shown in Fig. 6 and the data are summarized in Table XI.

It is not possible to say anything about the identity of the hyperfragment or its decay particles from their tracks. However, the visible energy release in this event is so low that it seems quite likely a π^{0} meson was emitted. Various assumptions were made for tracks 1 and 2 and the residual momentum given to a π^{0} meson. It was possible to fit the data by assuming tracks 1 and 2 were due to He^{3} and a triton, respectively, or vice versa. Then the hyperfragment decay was

$$_{\Lambda}\mathrm{Li}^{6}\rightarrow \mathrm{He}^{3}+t+\pi^{0}+Q,$$

where Q=24.1 or 25.6 Mev, and the binding of the Λ^{0} is

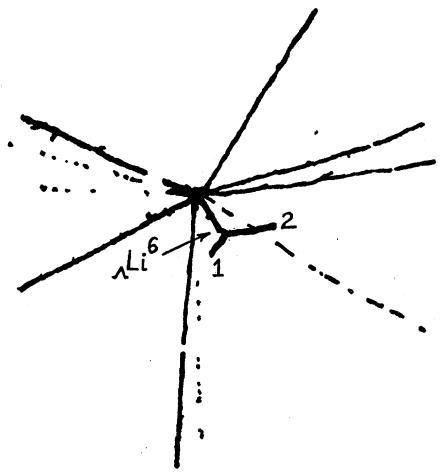

FIG. 6. Event 144 can be interpreted as the π^{0}-mesonic decay of $_{\Lambda}$Li^{6}. The hyperfragment came from a cosmic-ray star and had a range of only six microns. Tracks 1 and 2 were due to He^{3} and a triton, or vice versa.

5.8±1.5 Mev or 4.3±1.5 Mev. Of course, it is possible that this fit is fortuitous.

Event 161

In this event, which was produced by cosmic rays, the hyperfragment range is very long, 1310 microns. Its track indicates that it came to rest and that its charge was 4±1. As in event 144, the low visible energy release suggests that a π^{0} meson may have been emitted. If one of the tracks is assumed to have been produced by He^{4}, and the other by He^{3}, then the following scheme fits a hyperfragment decay:

$$_{\Lambda}\mathrm{Be}^{7}\rightarrow \mathrm{He}^{4}+\mathrm{He}^{3}+\pi^{0}+Q,$$

where Q=38.8±1.8 Mev if track 2 is He^{4} and 38.0±1.8 Mev if track 1 is He^{4}. Then the binding energy of the Λ^{0} is 8.3±1.8 Mev or 9.1±1.8 Mev. As pointed out before, such a fit may be fortuitous. The details of this event are given in Table XII.

TABLE XI. Data on event 144.

Track	Range in microns	Identity	Energy in Mev	Angle
Hyper-fragment	6	$_{\Lambda}$Li^{6}	3.3	
1	4.9	He^{3} or t	1.45 or 0.52	118°
2	5.3	t or He^{3}	0.57 or 1.58	

TABLE XII. Data on event 161.

Track	Range in microns	Identity	Energy in Mev	Angle
Hyper-fragment	1310	$_{\Lambda}$Be^{7}	194	
1	90.8	He^{3} or He^{4}	12.0 or 13.3	175.2°
2	92.3	He^{4} or He^{3}	13.5 or 12.1	

TABLE XIII. Events in which Λ^0 binding energies could be measured.[a]

Paper	Event number	Hyperfragment	Decay scheme	B_Λ (Mev)
II	87	${}_\Lambda H^3$	$d+p+\pi^-$	0.2±0 6
II	89	${}_\Lambda H^3$	$d+p+\pi^-$	−1.4±0.6
II	35	${}_\Lambda H^3$	$p+p+n+\pi^-$	0.2±0.6
II	70	${}_\Lambda H^4$	$p+d+n+\pi^-$	1.9±2.0 or 0.5±2.0
III	133	${}_\Lambda H^4$	$p+t+\pi^-$	1.8±0.4
I	4	${}_\Lambda He^4$	$p+t+\pi^0$	4.1±1.0
II	95	${}_\Lambda He^4$	$He^3+p+\pi^-$	0.0±2 0
II	90	${}_\Lambda He^4$	$He^3+p+\pi^-$	1.7±0.6
III	190	${}_\Lambda He^4$	$He^3+p+\pi^-$	2.3±0.6
III	213	${}_\Lambda He^4$	$p+d+n$	2.1±2.6
III	186	${}_\Lambda He^4$	$He^3+p+\pi^-$	3.2±0.6
		or ${}_\Lambda He^5$	$He^4+p+\pi^-$	3.2±0.6
III	188	${}_\Lambda He^4$	$He^3+p+\pi^-$	2.0±0.6
		or ${}_\Lambda He^5$	$He^4+p+\pi^-$	2.1±0.6
II	36	${}_\Lambda He^5$	$He^4+p+\pi^-$	1.7±0.6
III	211	${}_\Lambda He^5$	$He^4+p+\pi^-$	1.3±1.5
III	172	${}_\Lambda Li^6$	$p+d+d+n$	6.8±3.0
III	123	${}_\Lambda Li^6$	He^3+d+n	5.2±2.5
		or ${}_\Lambda Li^7$	He^4+d+n	5.0±2.5
III	164	${}_\Lambda Li^7$	$Li^6+p+\pi^-$	5.1±0.6
		or ${}_\Lambda Li^8$	$Li^7+p+\pi^-$	5.1±0.6
III	144	${}_\Lambda Li^6$	$He^3+t+\pi^0$	5.8±1.5 or 4.3±1.5
III	161	${}_\Lambda Be^7$	$He^4+He^3+\pi^0$	8.3±1.8 or 9.1±1.8
I	3	${}_\Lambda Be^7$	$He^4+p+p+n$	5.9±8.0
I	1	${}_\Lambda Be^8$	He^4+He^3+n	5.1±4.0
II	100	${}_\Lambda Be^9$	$Be^8+p+\pi^-$	6.3±0.6
I	2	${}_\Lambda C^{11}$	Li^7+He^3+p	13±6

[a] Binding energies of events previously reported in I and II were re-evaluated by using the new range-energy data of Barkas *et al.*[15] which were also used to calculate the binding energies of events reported in III.

C. Summary of Λ^0 Binding Energy Data

The hyperfragments which were reported in I and II were analyzed by using the range-energy relationship for π mesons and protons contained in the tables of Fay, Gottstein, and Hain.[18] Since then, more accurate measurements on the range-energy relationships of high-energy π mesons and low-energy protons have been reported by Barkas *et al.*[15] Therefore, all the hyperfragments reported in I and II were reanalyzed using the newer range-energy data. In most cases this led to a change of a few tenths of a Mev from the binding energies reported before. The corrected binding energies of the hyperfragments from I and II, and the binding energies of the hyperfragments reported in this paper, III, are listed in Table XIII. The average values of binding energies for various hyperfragments are summarized in Table XIV. In averaging, the individual values were weighted inversely proportional to the squares of their errors.

TABLE XIV. Average binding energies of hyperfragments.

Events	Hyperfragment	Average B_Λ (Mev)
87, 89, 35	${}_\Lambda H^3$	−0.3±0.4
133	${}_\Lambda H^4$	1.8±0.4
95, 90, 190, 213	${}_\Lambda He^4$	1.9±0.4
36, 211	${}_\Lambda He^5$	1.6±0.6
172	${}_\Lambda Li^6$	6.8±3.0
123	${}_\Lambda Li^6$ or ${}_\Lambda Li^7$	5.2±2.5 or 5.0±2.5
164	${}_\Lambda Li^7$ or ${}_\Lambda Li^8$	5.1±0.6
1	${}_\Lambda Be^8$	5.1±4.0
100	${}_\Lambda Be^9$	6.3±0.6
2	${}_\Lambda C^{11}$	13±6

[18] Fay, Gottstein, and Hain, Suppl. Nuovo cimento 11, 234 (1954).

D. Nonmesonic *vs* Mesonic Decays

Table XV gives the number of nonmesonic decays *vs* the number of π^--mesonic decays for hyperfragments of various charges (all the hyperfragments from I, II, and III are included). The ratios given should be taken as upper limits since the nonmesonic decays probably include some events due to slow π^- mesons. The number of nonmesonic decays would be expected to include some π^0-mesonic decays. For the case of $Z \geq 3$ the percentage of π^0 events included in the nonmesonic decays would most likely be very small since the nonmesonic mode of decay predominates. In the case of ${}_\Lambda He$ or ${}_\Lambda H$ however, the number of π^0-mesonic decays is not expected to be too small. Therefore the nonmesonic ${}_\Lambda He$ events must be examined to see how many could be due to π^0-mesonic decays. From an observation of π^--mesonic decays we would expect that in almost every case a π^0 decay of a helium hyperfragment, ${}_\Lambda He^A$, would be by the mode

$${}_\Lambda He^A \rightarrow He^{A-1}+n+\pi^0.$$

TABLE XV. Ratios of non-π^--mesonic to π^--mesonic decays.

Hyperfragment	Non-π^--mesonic / π^--mesonic
Hydrogen	0/6=0
Helium	18/7=2.6
Lithium	31/2=15.5
$Z>3$	140/2=70

In such an event the recoil would have a fairly short range, and therefore it would be very difficult to distinguish this event from a scattering. Therefore, it is not surprising that no such events are included among the 18 noncharged mesonic He hyperfragments, and it seems most likely that very few of the 18 events were π^0-mesonic decays.

All the non-π^--mesonic ${}_\Lambda He$ hyperfragments are listed in Table XVI, and the kinetic energy of the two charged decay products is given. In about half of the events the visible energy is considerably greater than the Q value for the free Λ^0 decay. In the others it was not possible to fit the data by the assumption that a π^0 meson was the only neutral particle emitted (except for event 4). If it is assumed that one neutron and a π^0 were emitted, then only events 108, 155, 169, and 171 could reasonably be interpreted as π^0-mesonic decays. Even for these it seems improbable that such is the case because the kinetic energy carried off by the neutron and π^0 is only about half of the total energy release, whereas they would be expected to carry off a large fraction of the kinetic energy.

From the above discussion it would seem reasonable to assume that about two of the 18 non-π^--mesonic events are π^0-mesonic, and therefore the ratio of non-mesonic to π^--mesonic decays for ${}_\Lambda$He is about 16/7.

DISCUSSION

No events have been found which can be interpreted as ${}_\Lambda H^2$. Their absence cannot be attributed to scanning bias because it is expected that the mode of decay would be

$$ {}_\Lambda H^2 \rightarrow p+p+\pi^-, $$

which would be extremely easy to detect. The absence of ${}_\Lambda H^2$ indicates the nonexistence of a bound state of the Λ^0-nucleon system. This might be expected from a consideration of the low binding energy of the Λ^0 particle in ${}_\Lambda H^3$. The data of Table XIII strongly suggest that this value is less than 0.5 Mev.

TABLE XVI. Helium hyperfragments which decayed without the emission of a π^- meson.

Event	Source of hyper-fragment[a]	Range of hyper-fragment[a] (μ)	Visible energy in decay[b] (Mev)	Remarks
4	3-Bev p	77	6.5	Can be interpreted as ${}_\Lambda He^4 \rightarrow p+t+\pi^0$
38	C.R.	4	23	Unlikely that a π^0 was emitted
61	3-Bev π^-	79	120	One proton of 100 Mev
74	3-Bev π^-	129	30	Very improbable that a π^0 was emitted
108	3-Bev π^-	2	15	Possible that a neutron and π^0 were emitted
115	3-Bev π^-	5	66	One proton of 64 Mev
120	3-Bev π^-	3	23	Unlikely that a π^0 was emitted
137	C.R.	635	74	One proton of 60 Mev
155	3-Bev π^-	55	19	Possible that a neutron and π^0 were emitted
169	C.R.	4	15	Possible that a neutron and π^0 were emitted
171	C.R.	6	11	Possible that a neutron and π^0 were emitted
202	K^- star	5	79	One proton of 42 Mev and one of 37 Mev
213	K^- star	1	110	Can be interpreted as ${}_\Lambda He^4 \rightarrow p+d+n$
215	K^- star	10	50	One proton of 48 Mev
219	K^- star	11	120	One proton of 80 Mev
220	K^- star	66	29	Very unlikely that a π^0 was emitted
221	K^- star	130	48	One proton of 46 Mev
223	K^- star	2	90	One proton of 84 Mev

[a] C.R. ≡cosmic ray.
[b] In all the events listed in this table two singly charged particles were emitted from the hyperfragment decay. The visible energy was obtained by assuming both to be protons. Some could have been deuterons or tritons.

It is still the case that no examples of ${}_\Lambda He^3$ have been found. It is considered quite unlikely that the mesonic decay of ${}_\Lambda He^3$ would be missed in scanning, for it would be a quite distinctive event, i.e.,

$$ {}_\Lambda He^3 \rightarrow p+p+p+\pi^-. $$

It seems most likely that ${}_\Lambda He^3$ is not bound. From the nonexistence of ${}_\Lambda He^3$ and the assumption of charge independence, $T=0$ can be assigned to the ground state of ${}_\Lambda H^3$. This assignment follows from the fact that the total binding of ${}_\Lambda H^3$ is greater than 2.2 Mev. If it were a $T=1$ state, the total binding energy of ${}_\Lambda He^3$ would be at least 1.5 Mev since the Coulomb energy of ${}_\Lambda He^3$ is surely not greater than that of He^3, which is 0.7 Mev. It also follows from the nonexistence of ${}_\Lambda He^3$ that the binding energy of ${}_\Lambda n^3$, if it exists, is less than something of the order of 0.7 Mev.

TABLE XVII. Nonmesonic to mesonic decay ratio, $Q^{(-)}$, for ${}_\Lambda He^4$ as a function of pion angular momentum, as given by Ruderman and Karplus.

l	0	1	2	3
$Q^{(-)}$ (B_Λ in Mev)	$0.4(B_\Lambda)^{\frac{1}{2}}$	$6.8(B_\Lambda)^{\frac{1}{2}}$	$120(B_\Lambda)^{\frac{1}{2}}$	$2000(B_\Lambda)^{\frac{1}{2}}$
Q^- for $B_\Lambda=2.0$ Mev	0.6	9.6	170	2800

The binding energies of 1.8 ± 0.4 Mev and 1.9 ± 0.4 Mev for ${}_\Lambda H^4$ and ${}_\Lambda He^4$ are consistent with the assumption that $T=\frac{1}{2}$ for the system of 3 nucleons and a Λ^0, and that charge independence is valid for hyperfragments. No other examples of complete charge multiplets have been identified.

The four ${}_\Lambda$Li events reported here make it clear that the binding energy of the Λ^0 in ${}_\Lambda$Li is considerably larger than it is in ${}_\Lambda$He. The binding in ${}_\Lambda$Li is about 5 Mev.

The binding energy data can be fitted to the assumption that the Λ^0 moves in an s state in a square well of range $\sim 1.2(A-1)^{\frac{1}{3}}\times 10^{-13}$ cm and a depth of about 20 Mev.

The data of Table XV shows that the nonmesonic mode of decay is rare for hydrogen hyperfragments, is comparable to the mesonic decay for helium, and strongly predominates for hyperfragments with $Z\geq 3$. Fowler[19] has shown that these data require that the lifetime for the mesonic mode of decay in nuclear matter must be much greater than the lifetime for the decay of a free Λ^0, and that the lifetime for the nonmesonic Λ^0 decay must be comparable to that of the free Λ^0 decay. The suppression of the mesonic mode of decay in nuclear matter may be due to the effect of the Pauli principle on the nucleon from the Λ^0 decay.

Ruderman and Karplus[4] have shown how to apply the data on the nonmesonic to mesonic decay ratios to a determination of the spin of the Λ^0 particle. Their results are summarized in Tables XVII and XVIII for ${}_\Lambda He^4$ and for hyperfragments of $Z>2$. The nonmesonic to mesonic decay ratios, $Q^{(-)}$, are given as a function

TABLE XVIII. Nonmesonic to mesonic decay ratio, $Q^{(-)}$, for hyperfragments of $Z>2$ as a function of pion angular momentum, as given by Ruderman and Karplus.

l	0	1	2	3
$Q^{(-)}$	4.8	80	1400	24000

[19] T. K. Fowler, Phys. Rev. **102**, 844 (1956).

TABLE XIX. Momenta, kinetic energies, and decay angles $\theta_{\Lambda\pi}$ for Λ^0 particles in hyperfragments.

Event	Hyperfragment	P_Λ (Mev/c)	E_Λ (Mev)	$\theta_{\Lambda\pi}$ [a] (degrees)	$\cos\theta_{\Lambda\pi}$
87	${}_\Lambda H^3$	103	4.8	34	0.83
89	${}_\Lambda H^3$	72	2.3	170	−0.98
143	${}_\Lambda H^3$ or ${}_\Lambda H^4$	16	0.1	78	0.22
133	${}_\Lambda H^4$	165	12.1	100	−0.17
90	${}_\Lambda He^4$	57	1.4	166	−0.97
95	${}_\Lambda He^4$	84	3.1	30	0.87
190	${}_\Lambda He^4$	106	5.6	29	0.87
186	${}_\Lambda He^4$ or ${}_\Lambda He^5$	69	2.2	107	−0.29
188	${}_\Lambda He^4$ or ${}_\Lambda He^5$	40	0.7	35	0.82
36	${}_\Lambda He^5$	131	7.7	44	0.72
211	${}_\Lambda He^5$	121	6.6	155	−0.90
164	${}_\Lambda Li^7$ or ${}_\Lambda Li^8$	44	0.9	77	0.21
167	${}_\Lambda Li^7$ or ${}_\Lambda Li^8$	117	6.1	162	−0.95
100	${}_\Lambda Be^9$	145	9.5	24	0.91

[a] $\theta_{\Lambda\pi}$ is the angle in the Λ^0 center-of-mass system between the direction of motion of the π meson from the Λ^0 decay and the line of flight of the Λ.

of the angular momentum of the pion from the decay $\Lambda^0 \rightarrow p+\pi^-$.

If we assume that $\Lambda^0 \rightarrow n+\pi^0$ occurs half as frequently as $\Lambda^0 \rightarrow p+\pi^-$ (this is the case if the Λ^0 decay is a transition from isotopic spin $T=0$ to $T=\frac{1}{2}$), then since $Q^{(0)} \sim Q^{(-)}$,[4] where $Q^{(0)}$ is the nonmesonic to mesonic ratio for the mode $\Lambda^0 \rightarrow n+\pi^0$, we would expect that $\frac{1}{3}$ of the 16 nonmesonic ${}_\Lambda He$ decays would be due to the conversion of a neutral pion. Hence $Q^{(-)}=\frac{2}{3}(16/7)=1.5$. This value of $Q^{(-)}$ is measured for a mixture of ${}_\Lambda He^4$ and ${}_\Lambda He^5$ hyperfragments whereas the results of Table XVII are for ${}_\Lambda He^4$. However, since the binding of the Λ^0 in ${}_\Lambda He^5$ appears to be not much different than in ${}_\Lambda He^4$, Table XVII should also be a good approximation for ${}_\Lambda He^5$.

In the results of Table XVIII for heavy hyperfragments, Ruderman and Karplus have taken into account the fact that π^0-mesonic decays in most cases would be interpreted as nonmesonic decays. Hence $Q^{(-)}$ for hyperfragments of $Z>2$ can be found directly from Table XV and is $171/4 \approx 43$.

Both for ${}_\Lambda He$ and the heavier hyperfragments the observed value of $Q^{(-)}$ is intermediate between the values expected for $l=0$ and $l=1$. Thus the data indicate a spin of $\frac{1}{2}$ or $\frac{3}{2}$ for the Λ^0. The intermediate values of $Q^{(-)}$ could be the result of insufficient experimental data or approximations used in the theoretical calculations. Another possibility of great interest is that the Λ^0 may be a parity doublet, one member of which decays into an $l=0$ state, and the other into an $l=1$ state. Then it would be quite conceivable that $Q^{(-)}$ should be intermediate between the expected values for $l=0$ and $l=1$ in Tables XVII and XVIII. The effect of a Λ^0 parity doublet on the nonmesonic to mesonic decay ratios has been discussed by Treiman.[7]

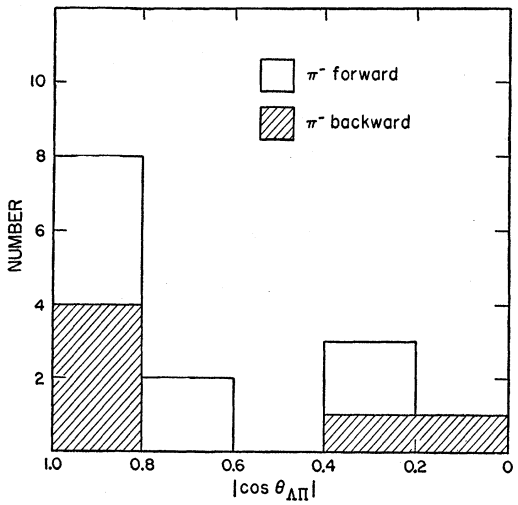

FIG. 7. Angular distribution of 14 cases of Λ decays from hyperfragments reported in I, II, and III and enumerated in Table XIX.

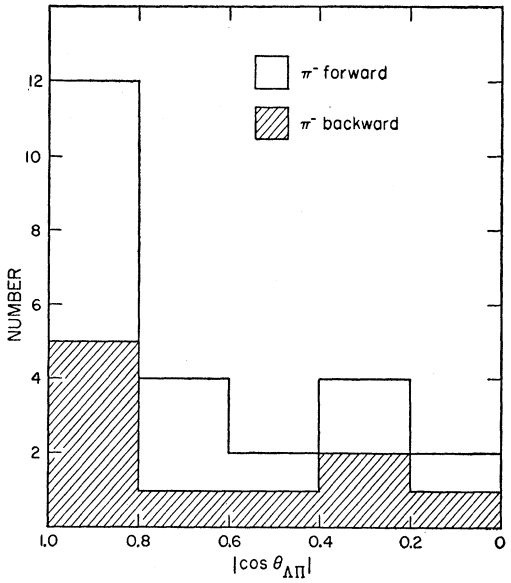

FIG. 8. Angular distribution of 24 cases of Λ decays from hyperfragments which include the 14 enumerated in Table XIX plus 10 reported by Zielinski.[8]

As was pointed out in II, it may be reasonable, in view of the low Λ^0 binding energy, to assume that in mesonic decays the proton and π^- meson do not interact with the residual nucleus. Then the momentum of the Λ^0 within the hyperfragment is simply given by the vector sum of the momentum of the π^- meson and proton. Zielinski[8] has pointed out that using this approach we can also obtain the angle $\theta_{\Lambda\pi}$, in the Λ^0-particle rest frame, between the direction of motion of the decay π meson and the line of flight of the Λ^0. Table XIX lists the kinetic energy and momentum of the Λ^0 within the hyperfragment, and the angle $\theta_{\Lambda\pi}$, for such events. Figure 7 is a histogram of the frequency distribution of the 14 decay angles given in Table XIX. Zielinski, in his paper, gave this frequency distribution

for 16 cases obtained from various laboratories and including the six events reported in II. If the eight cases reported in this paper are added to his distribution, this gives the histogram of Fig. 8 for 24 events. Of the 24 events, 14 decay with the π forward and 10 with the π backward. Hence no statement can be made as to a possible forward-backward asymmetry. However, there does appear to be a significant peaking in the forward and backward directions. The probability (from a chi-square test) that the histograms of Figs. 7 and 8 could result from an isotropic distribution is about one percent.

If the assumption that the proton and π meson do not interact with the residual nucleus is correct, then a possible explanation for this angular distribution would be that the spin of the Λ^0 is greater than $\frac{1}{2}$. The results on the nonmesonic *vs* mesonic decay ratios, however, make it appear unlikely that the spin is greater than $\frac{3}{2}$, and infer that if the spin is $\frac{3}{2}$ the parity of the Λ^0 is the same as that of the proton.

It is to be noted that certain events, namely numbers 4, 144, and 161 are strongly indicative that the decay mode $\Lambda^0 \rightarrow n+\pi^0$ does indeed occur, although in general it is difficult to detect. We also point out that decay modes such as $\Lambda^0 \rightarrow p+e^-+\nu$ or $\Lambda^0 \rightarrow p+\mu^-+\nu$ would be easily detectable in emulsion if hyperfragments should decay by them. No examples of these were seen out of 17 π^--mesonic hyperfragment decays.

No examples of decays in flight of hyperfragments were found in this study. The total moderation time of all the hyperfragments in I, II, and III is of the order of the lifetime of the free Λ^0. Hence it appears that the lifetime of the Λ^0 particle is not appreciably shortened in hyperfragments.

ACKNOWLEDGMENTS

The authors are indebted to Professor E. J. Lofgren and many other physicists at Berkeley for their help in making the exposures. The cosmic-ray plates were exposed for us by Major David G. Simons, United States Air Force, for which we are very grateful. Many discussions with Professor R. G. Sachs, Professor J. K. Knipp, Professor S. B. Treiman, and Professor G. A. Snow were helpful and stimulating.

Note added in proof.—The authors have recently received from Dr. M. Ruderman and Dr. R. Karplus a revised calculation of the nonmesonic to mesonic decay ratios as a function of pion angular momentum. The values for $Q^{(-)}$ quoted in Tables XVII and XVIII represent minimum values and hence determine an upper limit for the spin of the Λ^0. A better estimate for the values of $Q^{(-)}$ was made by including the following modifications: (a) A factor 1.7 comes from using the nuclear density obtained by electron scattering. (b) A factor 5 comes from Primakoff's more accurate treatment of the exclusion principle in heavier fragments. (c) A factor greater than one comes from positive position correlations from the Λ^0-N attraction. The revised values of $Q^{(-)}$ are given in Table XX for ${}_\Lambda\mathrm{He}$ and in Table XXI for hyperfragments of $Z \geqslant 3$.

TABLE XX. Revised estimate for $Q^{(-)}$ as a function of pion angular momentum for ${}_\Lambda\mathrm{He}^4$.

l	0	1	2	3
$Q^{(-)}$	$0.8B_\Lambda^{\frac{1}{2}}$	$14B_\Lambda^{\frac{1}{2}}$	$240B_\Lambda^{\frac{1}{2}}$	$4000B_\Lambda^{\frac{1}{2}}$
for $B_\Lambda=2.0$ Mev	1.1	20	340	5600

A comparison of the data with these revised values strongly indicates that the S-wave pion predominates and hence that the spin of the Λ^0 is $\frac{1}{2}$. There may be some P-wave contribution if parity is not conserved in the Λ^0 decay.

TABLE XXI. Revised estimate for $Q^{(-)}$ as a function of pion angular momentum for hyperfragments of $Z \geqslant 3$.

l	0	1	2	3
$Q^{(-)}$	50	800	14 000	240 000

Since the evidence that the spin of the Λ^0 is $\frac{1}{2}$ seems strong, we must look for a reason other than a high spin to explain the anisotropy of Fig. 8. Dr. R. Gatto has pointed out to us that it may be possible that this effect is indeed the result of the interaction of the final particles with the residual nucleus. In fact since the Λ^0 stays mainly outside the nucleus, it might be expected that the reabsorption cuts out a contribution mainly from angles of about 90°.

We are pleased to thank Dr. Ruderman and Dr. Karplus for sending us their revised calculations, and Dr. Gatto for an enlightening communication.